REPORT DOCUMENTATION PAGE

1. REPORT DATE *(DD-MM-YYYY)*	2. REPORT TYPE	3. DATES COVERED *(From - To)*
06-06-2005	Conference Proceedings (not refereed)	

4. TITLE AND SUBTITLE	5a. CONTRACT NUMBER
The Influence of Swell on the Sea Surface Roughness and the Growth of Wind Waves	
	5b. GRANT NUMBER
	5c. PROGRAM ELEMENT NUMBER
	0602435N

6. AUTHOR(S)	5d. PROJECT NUMBER
Chen, Qin, Hwang, Paul A., Kaihatu, James A.	
	5e. TASK NUMBER
	5f. WORK UNIT NUMBER
	73-M125-04

7. PERFORMING ORGANIZATION NAME(S) AND ADDRESS(ES)	8. PERFORMING ORGANIZATION REPORT NUMBER
Naval Research Laboratory Oceanography Division Stennis Space Center, MS 39529-5004	NRL/PP/7330--04-5030

9. SPONSORING/MONITORING AGENCY NAME(S) AND ADDRESS(ES)	10. SPONSOR/MONITOR'S ACRONYM(S)
Office of Naval Research 800 N. Quincy St. Arlington, VA 22217-5660	ONR
	11. SPONSOR/MONITOR'S REPORT NUMBER(S)

12. DISTRIBUTION/AVAILABILITY STATEMENT

13. SUPPLEMENTARY NOTES

14. ABSTRACT

The paper utilizes an extended Boussinesq wave model incorporating the wind forcing to examine the effects of swell on the spatial variation of the sea surface roughness and the growth of wind waves. We first introduce the new parameterization of the momentum flux transferred from the wind to surface gravity waves followed by an analysis of the effect of wave nonlinearity on the drag coefficient using Stokes' second-order wave theory. The time-domain Boussinesq wave model with the wind forcing is tested against the field measurements of wave growth rate in a shallow lake. Fairly good agreement between modeled and measured wave heights is obtained. Numerical experiments are then carried out to test a hypothesis for the suppression of the wave growth rate by the following swell. A simple mechanism is suggested to explain the influence of swell on the short waves observed in the numerical and laboratory experiments.

15. SUBJECT TERMS

Bossinesq wave model; sea surface roughness; parameterization of momentum flux; Heterogeneous Air-Sea Momentum Flux; wave nonlinearity; drag coefficient; wave growth

16. SECURITY CLASSIFICATION OF:			17. LIMITATION OF ABSTRACT	18. NUMBER OF PAGES	19a. NAME OF RESPONSIBLE PERSON
a. REPORT	b. ABSTRACT	c. THIS PAGE	UL	7	Paul A. Hwang
Unclassified	Unclassified	Unclassified			19b. TELEPHONE NUMBER *(Include area code)*
					228-688-4708

Proceedings of the 29th International Conference

Coastal
Engineering
2004

Vol. 1

THE INFLUENCE OF SWELL ON THE SEA SURFACE ROUGHNESS AND THE GROWTH OF WIND WAVES

QIN CHEN

Department of Civil Engineering, University of South Alabama
Mobile, AL 36688, USA

PAUL A. HWANG

Oceanography Division, Naval Research Laboratory
Stennis Space Center, MS 39529-5004, USA

JAMES M. KAIHATU

Oceanography Division, Naval Research Laboratory
Stennis Space Center, MS 39529-5004, USA

The paper utilizes an extended Boussinesq wave model incorporating the wind forcing to examine the effects of swell on the spatial variation of the sea surface roughness and the growth of wind waves. We first introduce the new parameterization of the momentum flux transferred from the wind to surface gravity waves followed by an analysis of the effect of wave nonlinearity on the drag coefficient using Stokes' second-order wave theory. The time-domain Boussinesq wave model with the wind forcing is tested against the field measurements of wave growth rate in a shallow lake. Fairly good agreement between modeled and measured wave heights is obtained. Numerical experiments are then carried out to test a hypothesis for the suppression of the wave growth rate by the following swell. A simple mechanism is suggested to explain the influence of swell on the short waves observed in the numerical and laboratory experiments.

1. Introduction

It is well known that many physical processes occurring at the air-sea interface, such as air-sea mass, momentum and energy exchanges, are controlled by the ocean surface roughness that has often been characterized in the literature as being homogeneous in space and time from a large-scale point of view. Recently, it is realized, however, that the utilization of remote sensing techniques in the study of the air-sea interface requires an in-depth understanding of the spatial and temporal variability of the ocean surface roughness at multiple scales.

The ocean surface roughness is indeed inhomogeneous within a wavelength. The surface areas on wave crests are usually rougher than those on wave troughs. The mechanisms range from capillary ripples on wave crests to larger scale wave breaking (see e.g., Longuet-Higgins, 1963; Jiang et al., 1999; Ducan et al., 1999). An ambient swell or current can also cause significant spatial variations of the surface roughness as short waves become steeper on the swell crest than

those on the swell trough (Longuet-Higgins and Stewart, 1960), as demonstrated by Hwang's (1999 and 2002) laboratory measurements and analyses. The purpose of the study is to quantify the effects of swell on the spatial variability of the ocean surface roughness and the growth of wind waves using a phase-resolving numerical wave model with the wind forcing.

The paper is organized as follows. First, we present the new parameterization of the momentum flux transferred from the wind to surface gravity waves. Next, we analyze the effect of wave nonlinearity on the drag coefficient using Stokes' second-order wave theory. After that, the implementation of the parameterized wind stress into a phase resolving Boussinesq wave model with enhanced dispersion properties is briefly discussed. Then tests of the extended Boussinesq model with the wind forcing against wave measurements in a shallow lake are carried out followed by a series of numerical experiments on the sea-swell-wind interactions. Finally, we summarize the findings of the study.

2. Heterogeneous Air-Sea Momentum Flux

2.1. *Parameterization of Momentum Flux*

The momentum flux transferred from wind to surface waves in a time-domain Boussinesq wave model may be parameterized as the wind stress, $\tau = \rho_a\, C_d\, U |U|$, where U is the wind velocity vector at a reference elevation, ρ_a is the air density, and C_d is the corresponding drag coefficient. Suggested by the field evidence, the wind drag coefficient in the nearshore must be a function of not only the wind speed, but also the geometry of the surface gravity waves that are often skewed and asymmetrical owing to the seabed boundary. We adopt Chen et al.'s (2004) formula of phase-resolving drag coefficient as follows.

$$C_d 10^3 = (a_1 + a_2\, |\,\eta_x\,|) + bU_{10} \qquad (1)$$

where $a_1 = 0.2$, $a_2 = 18$ and $b = 0.065$ are empirical coefficients, and η_x is the instantaneous surface slope computed in the Boussinesq model. Phase average of the drag coefficient allows for a comparison of the new formula with conventional drag coefficient formulas. Figure 2 shows the comparison of the new formula with the existing empirical formulas for the drag coefficient proposed in the literature (see e.g. Geernaert, 1990). Each formula represents the best fit to a specific dataset. It is seen that the scattering of the drag coefficient as a function of the wind speed may be explained by the effect of the sea state, or the wave steepness, ka (k = wave number and a = wave amplitude), ranging from 0.05 to 0.2 with an increment of 0.05. Statistically, Eq. (1) agrees fairly well with all the data, which is not achieved by any single existing formula of drag coefficient. The third term in Eq. (1) is set to be a constant for a weak wind.

$$\tau = C_d \rho_a |U_{10} - C|(U_{10} - C) \qquad (2)$$

where C is the instantaneous wave celerity estimated in the Boussinesq model. Equation (2) is similar to the wind stress formulation followed by Schwab et al. (1984) in a wave prediction model on the basis of a phase-averaged momentum balance equation rather than an energy balance equation.

2.2. Effects of Wave Nonlinearity on the Drag Coefficient

The phase-resolving wind drag coefficient depends on the wave steepness and becomes effective only on the wave crest. It is well known that the effects of wave nonlinearity increase the wave steepness and result in peaky wave profiles. We shall analyze the effect of wave nonlinearity on the drag coefficient given by Eq. (1) using Stokes' second-order wave theory.

The free surface profile given by Stokes' second-order theory reads

$$\eta = a\cos(kx - \omega t) + \frac{a^2 k}{4}\frac{(2 + \cosh 2kh)\cosh kh}{\sinh^3 kh}\cos 2(kx - \omega t) \qquad (3)$$

where a is the first-order (linear) amplitude of the free-surface disturbance, $k = 2\pi/L$ is the wave number, L is the wave length, x is the horizontal distance, t is time, and ω is the angular frequency. At $t = 0$ and in the deep water ($h>>L/2$), Eq. (3) may be simplified as

$$\eta = a\cos kx + \frac{a^2 k}{2}\cos 2kx \qquad (4)$$

Upon the use of the trigonometric identity and rearrangement of Eq. (4), we obtain

$$\eta k = a^2 k^2 \cos^2 kx + ak\cos kx - \frac{a^2 k^2}{2} \qquad (5)$$

Because the wind stress (or drag coefficient) is only applied on the wave crest above the still water level, we need to find out the length of the wave crest. Solving Eq. (5) with $\eta k = 0$ yields

$$x_0 k = \arccos[f(ak)] \qquad (6)$$

in which

$$f(ak) = -\frac{1}{2ak} + \sqrt{\left(\frac{1}{2ak}\right)^2 + \frac{1}{2}} \qquad (7)$$

Integrating the drag coefficient over a wave length leads to the phase-averaged drag coefficient

$$\overline{C}_d = \frac{1}{L}\int_{-x_0}^{l+x_0} C_d dx = \frac{a_1}{\pi}kx_0 + \frac{a_2}{\pi}k\eta_{max} + \frac{b}{\pi}kx_0 U_{10} \qquad (8)$$

where η_{max} is the surface elevation at the wave crest. For linear waves, we have

One of the crucial differences in airflow over steep surface waves in comparison to the flow over a flat surface is the presence of a form drag due to the Bernoulli effects and separation of airflow. Laboratory measurements of the tangential and normal stresses on the air-water interface (Banner and Peirson, 1998) suggest that the form drag accounts for the major proportion of the wind stress once the waves have developed beyond their early growth stage. The most interesting scenario of wind effects on coastal waves is the strong wind condition. We hypothesize that the form drag is a dominant contributor to the momentum flux between the atmosphere and the nearshore wave field. The hypothesis is in line with the sheltering theory proposed by Jeffreys (1925) as a mechanism of wave generation.
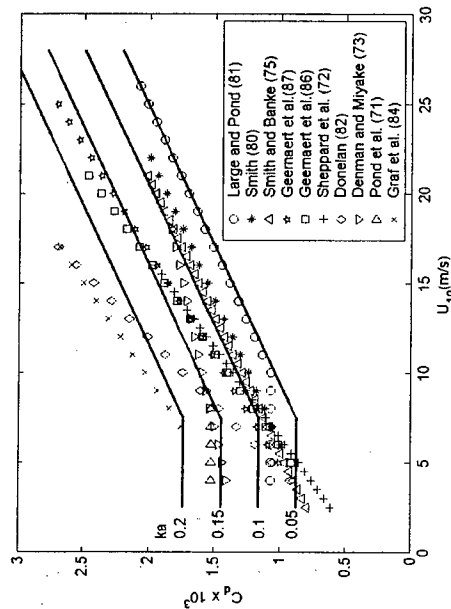

Figure 1. Comparison of Equation (1) with the drag coefficient formulas compiled by Geernaert (1990).

The time-domain Boussinesq model resolves the individual wave motion and predicts reasonably well the geometry of the surface waves distorted by the seabed, such as the skewness and asymmetry of the waves in the shallow water (e.g. Chen et al., 2000 and Shi et al. 2003). The wind stress implemented into the Boussinesq model should vary over a wavelength, with a larger drag coefficient on the wave crest than that in the trough to take the form drag into account. In fact, only the heterogeneous distribution of the wind stress over a wavelength allows for changes of wave height by a wind in a phase-resolving wave model. Assuming that the form drag is dominant over the skin friction, we apply the wind stress on the wave crest only, neglecting the effect of the shear stress on the wave trough in the Boussinesq model. With the instantaneous wave celerity and wave slope obtained from the computed surface elevation at each grid and every time step, the wind stress is calculated as a function of the wind velocity relative to the wave celerity as well as the wave slope in the following form

$x_0 = L/4$ and $\eta_{max} = a$. The ratio of the drag coefficient on a Stokes' second-order wave profile to that on a linear wave profile is given by

$$\frac{\overline{C}_d}{(\overline{C}_d)_{linear}} = 1 + \frac{(a_1 + bU_{10})(2kx_0 - \pi) + a_2(ka)^2}{(a_1 + bU_{10})\pi + 2a_2 ka} \quad (9)$$

Figure 2 illustrates the variation of such a ratio as a function of wave steepness and wind speed. It is seen that the wave nonlinearity can increase the phase-averaged drag coefficient by 10-15 percent.
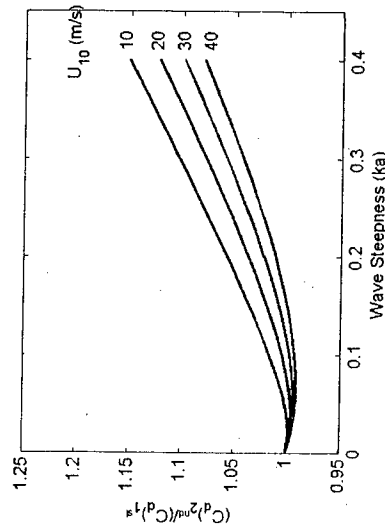

Figure 2. Effects of wave steepness and wind speed on the drag coefficient

2.3. A Boussinesq Wave Model with Wind Forcing

The phase-resolving formulation of the wind stress has been implemented into a Boussinesq wave model by Chen et al. (2004). In order to take into account the short waves generated by local winds, the dispersion accuracy of the one-dimensional version of the model has been extended to $kh = 6$ ($h = $ still water depth) by introducing the additional terms from Madsen and Schäffer's (1998) equations into the model. A new set of coefficients for better shoaling properties of the equations (Madsen, 2002, personal communication, and Kennedy et al, 2002) has also been implemented into the model. In one horizontal dimension, the extended Boussinesq equations read

$$\eta_t + M_x = 0 \quad (10)$$

and

$$u_{\alpha t} + u_\alpha u_{\alpha x} + g\eta_x + \Lambda - R_h - R_s + R_f - R_w = 0 \quad (11)$$

where M represents the volume rate of flow and Λ denotes all the dispersive terms. In the equations, η is the free surface elevation relative to the still water

level; u_α is the velocity at the reference elevation z_α ($= -0.54122h$) in the water column; and the subscripts t and x denote time and spatial differentiations, respectively. The additional terms, $R_h, R_s, R_f,$ and R_w represent the effects of wave breaking, subgrid lateral turbulent mixing, seabed shear stress, and wind stress, respectively. Detailed descriptions of the first three terms can be found in Chen et al. (1999). Upon the use of Eq. (2), we obtain

$$R_w = \frac{\rho_a}{\rho(h+\eta)} C_d |U_{10} - C|(U_{10} - C) \quad (12)$$

where ρ is the water density. The internal wave-maker for the generation of random waves at the offshore boundary is extended to accommodate the enhancement of dispersion properties in the Boussinesq equations. Other extensions of the model include the modification of the breaking criteria in the model to account for the energy dissipation owing to whitecaps.

3. Modeling Wave Growth on a Shallow Lake

Can the wind stress implemented into the Boussinesq model simulate the growth of wind waves over a long fetch with a non-zero up-wave boundary condition? We shall address such a question using the data set of wave growth in Lake George, Australia collected by Young and Verhagen (1996).

Lake George is a shallow lake with a typical water depth of 2m. It is about 20km long and 10km wide. A series of eight observation stations were deployed along the north-south fetch to measure the wind waves. The wave data collected by Young and Verhagen (1996) under a nearly ideal condition have served as a test bed for a number of phase-averaged wave models, such as SWAN (Simulating WAves Nearshore, Booij et al., 1999). We choose two data sets corresponding to a medium wind speed of $U_{10} = 10.8$m/s and a higher wind speed of $U_{10} = 15.2$m/s to test the wind stress formulation incorporated into the Boussinesq model. Owing to the dispersion limit of the Boussinesq model ($kh < 6$), only the observations at the last four stations (5-8) are utilized. The fetch between Stations 5 and 8 is about 4.25 km. The up-wave boundary condition is taken from the observation at Station 5 where the zero-moment wave height is 0.367m and the peak wave period is 2.34s in the case of a moderate wind ($U_{10} = 10.8$m/s), and 0.473m and 2.4s in the case of a strong wind ($U_{10} = 15.2$m/s).We use TMA shallow water wave spectra (Bouws et al., 1985) with the shape parameter $\gamma = 3.3$ at the up-wave boundary as the input to the Boussinesq model. A bottom friction coefficient of $f = 0.0005$ is used in the quadratic law of the bed shear stress that utilizes the velocity near the mid depth (Chen et al., 1999).
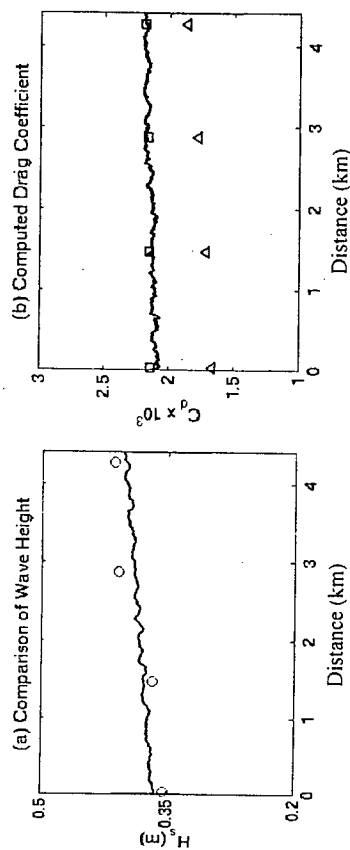
Figure 3. Comparisons of the computed and measured significant wave heights (top), and the computed and inferred drag coefficients (bottom) in the case of $U_{10} = 10.8$m/s. Solid lines: Boussinesq model results, circles: Young and Verhagen's (1996) observations, squares: Anctil and Donelan (1996), and triangles: Taylor and Yelland (2001).

Figure 3 shows comparisons of the computed and measured significant wave heights as well as the computed and inferred drag coefficients under the moderate wind condition. It is seen that the wave heights predicted by the Boussinesq model are in fairly good agreement with the field measurements. The computed peak wave periods, however, do not agree with the observations (not shown here). The wind stress incorporated into the Boussinesq model simply does not lead to the increase of wave period along the fetch. The downshift of the peak frequency is absent in the modeled wave energy spectrum. This is attributed to the inability of the present Boussinesq model to take quadruplet interactions into account. Interestingly, the phase-averaged drag coefficient calculated from the Boussinesq model is in good agreement with the coefficient estimated using the modeled wave characteristics and Anctil and Donelan's (1996) formula. The drag coefficients given by Taylor and Yelland's (2001) formula (triangles), however, are smaller than either Boussinesq or Anctil and Donelan's result (solid line and squares).

Similar comparisons are made for the case of high wind speed as shown in Figure 4. Again, the Boussinesq model predicts the growth of wave height fairly well in comparison to the field measurements, but considerably under-predicts the increase of wave period (not shown here). The agreement among the drag coefficients is also very similar to the case with a moderate wind. The phase-averaged drag coefficient obtained from the Boussinesq model agrees better with Anctil and Donelan's result than does Taylor and Yelland's formula, as shown in Figure 4b. Notice that all the drag coefficients are computed using the wave field given by the one-dimensional Boussinesq model, which is not able to predict the downshift of the peak frequency. Nevertheless, the prediction of wave height growth under both moderate and strong wind conditions by the Boussinesq model confirms that the new formulation of wind stress is a reasonably good representation of the momentum flux transferred from a wind to surface waves in a phase-resolving model.

4. The Influence of Swell on the Growth of Wind Waves

Donelan (1987) among others has found that the addition of mechanically-generated swell to the wind waves in a wave flume results in a pronounced reduction in the energy of the wind sea while the swell gains significant energy from the following wind in comparison to pure wind waves. Although a number of hypotheses have been proposed in the literature, the attenuation mechanism for the wind sea owing to the presence of swell is still poorly understood. As demonstrated in the preceding section, the extended Boussinesq model is able to simulate the growth of wave energy for a given wind speed and a non-zero wave spectrum at the up-wave boundary. We shall conduct a series of numerical experiments to examine how swell influences the growth rate of wind waves on the basis of the extended Boussinesq wave model with the wind forcing. The Lake George case with a moderate wind is used as a reference for comparison.
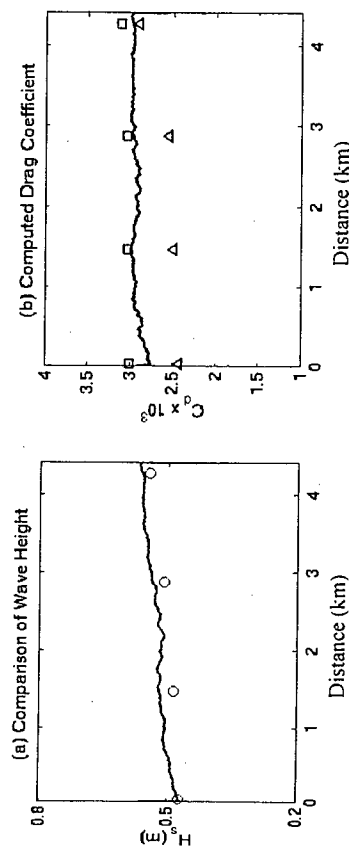
Figure 4. Comparisons of the computed and measured significant wave heights (a) as well as the computed and inferred drag coefficients.(b) in the case of $U_{10} = 15.2$m/s. Solid lines: Boussinesq model results, circles: Young and Verhagen's (1996) observations, squares: Anctil and Donelan (1996), and triangles: Taylor and Yelland (2001).

Figure 5 depicts snapshots of the computed free surface elevations of the cases with and without swell. The right panel corresponds to the first case with a moderate wind speed in the preceding section. A monochromatic, long wave train with a period of three times the peak wave period of the short waves is imposed at the up-wave boundary. The wave height of the swell is 0.184 m. Each snapshot in the right panel. The wave height of the swell is 0.184 m. Each snapshot (e.g. A to F) in each panel is 15 minutes apart, beginning 15 minutes after the model starts.

Figure 6 shows the energy density spectra of the modeled sea surface with and without swell. The dashed lines represent the spectra at the up-wave boundary while the solid lines are the spectra 4 km down-wind. In contrast to the spectra of the pure wind waves on the right, the left panel shows that the short waves barely grow while the swell gains energy from the wind. The Boussinesq model qualitatively reproduces what Donelan (1987) observed in the laboratory about the suppression of the wave growth rate in the presence swell under field conditions. No field measurements of sea-swell interaction, however, are available for a direct test of the influence of swell predicted by the Boussinesq wave model with the wind forcing.
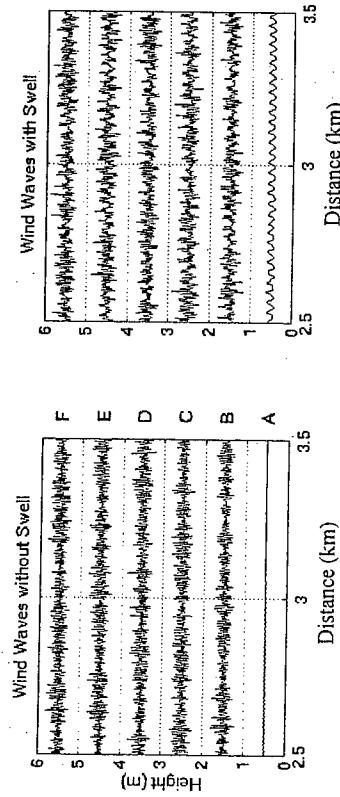

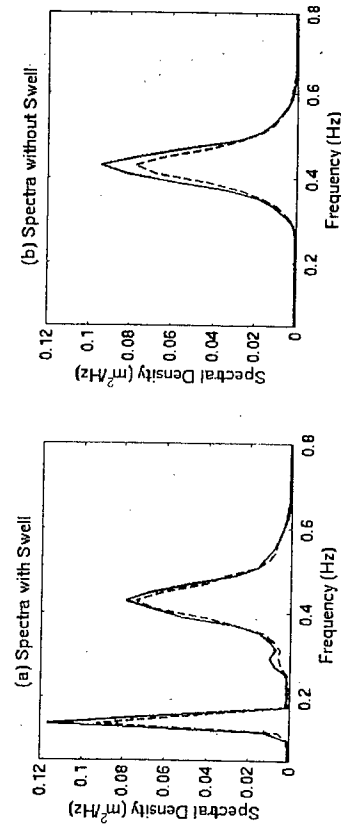Figure 5. Snapshots of modeled sea surface without (left) and with (right) swell

Figure 6. Suppression of wave growth by the ambient swell (left). Dashed lines: up-wave boundary, solid lines: 4 km down-wave.

The slope of the sea surface is a measure of the surface roughness. Figure 7 illustrates spectra of the modeled sea surface slope with and without swell. The dashed lines represent the slope spectra at the up-wave boundary while the solid

lines are the spectra 4 km down-wind. A comparison of the left and right panels shows that the swell actually reduces the growth rate of the surface slope, or the sea surface roughness of the short waves. This is consistent with the suppression of the short-wave energy growth rate by the following swell.

Figure 8 depicts the spatial variations of the wave height and phase-averaged drag coefficient with and without swell. The solid lines denote the model result of pure wind waves while the dashed lines are the result of combined sea and swell. It is seen that the presence of swell yields a slightly smaller growth rate of the total wave energy than that of the pure sea. A similar trend is found in the phase-averaged drag coefficient, as shown on the right.
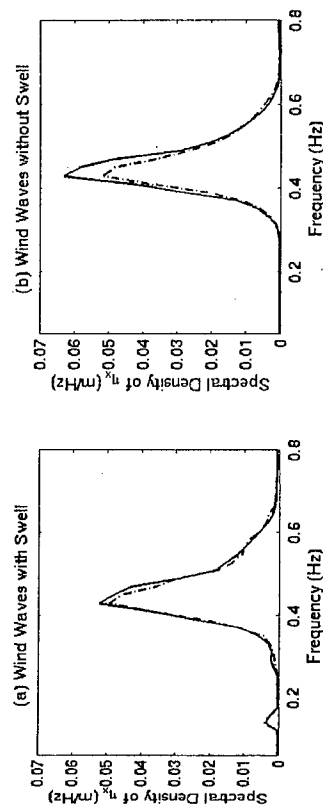

Figure 7. Spectra of sea surface slope with (left) and without (right) swell. Dashed lines: up-wave boundary, solid lines: 4 km down-wave.
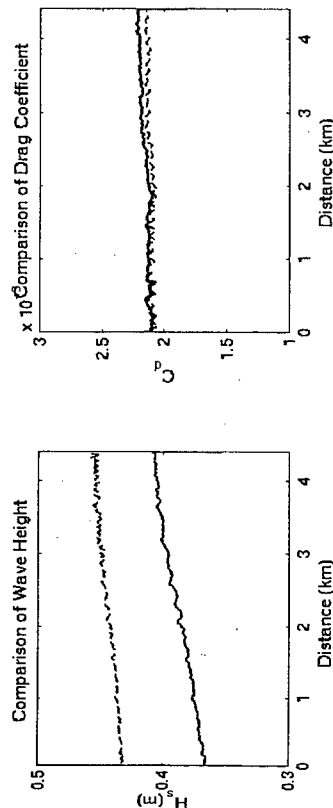

Figure 8. Effects of swell on wave height and drag coefficient. Dashed lines: sea and swell. solid lines: short waves.

To examine the effect of the swell steepness on the growth rate of the wind waves, we reduce the swell amplitude to 0.041 m, and repeat the simulation above without changing other conditions. The Boussinesq model predicts that the smaller the swell steepness, the less degree the suppression of the shore-wave growth rate, as seen by a direct comparison of Figure 6 and Figure 9.

interactions and wind effects on nearshore wave propagation. However, the limit of the dispersion accuracy to $kh < 6$ prevents the extended Boussinesq wave model from being compared directly with existing laboratory datasets on the influence of swell on the growth of wind waves. Thus, it is recommended that state-of-the-art Boussinesq models with the dispersion accuracy up $kh = 40$ (e.g. Madsen et al., 2002) be employed for the study of sea-swell-wind interactions in the future.

References

Anctil, F., and Donelan, M. A. (1996). Air-water momentum flux observations over shoaling waves. *J. Phys. Oceanogr.* 26: 1344-1353.

Banner, M. L., and Peirson, W. L. (1998). Tangential stress beneath wind driven air-water interfaces. *J. Fluid Mech.*, 364, 115-145.

Booij, N., Ris, R. C., and Holthuijsen, L. H. (1999). A third-generation wave model for coastal regions. Part 1, Model description and validation. *J. Geophys. Res.*, C4, 104, 7649-7666.

Bouws, E., Gunther, H., Rosenthal, W., and Vincent, C. L. (1985). Similarity of the wind wave spectrum in finite depth water. *J. Geophys. Res.*, 90, 975-986.

Chen, Q., Dalrymple, R. A., Kirby, K. T., Kennedy, A. B., and Haller, M. C. (1999). Boussinesq modeling of a rip current system. *J. Geophys. Res*, 104 (C9), 20,617-20,637.

Chen, Q., Kirby, J. T., Dalrymple, R. A., Kennedy, A. B., and Chawla, A. (2000). Boussinesq modeling of wave transformation, breaking and runup. II: 2D. *Journal of Waterway, Port, Coastal and Ocean Engineering*, 126, 48-56.

Chen, Q., Kaihatu, J. M. and Hwang, P. A., (2004). Incorporation of the wind effects into Boussinesq wave models. *Journal of Waterway, Port, Coastal and Ocean Engineering*, 130, 312-321.

Donelan, M. A. (1987). The effect of swell on the growth of wind waves. *Johns Hopkins APL Technical Digest*, 8 (1), 18-23.

Duncan, J. H., Qiao, H., Philomin, V. and Wenz, A., (1999). Gentle spilling breakers: crest profile evolution. *J. Fluid Mech.*, 379, 191-222.
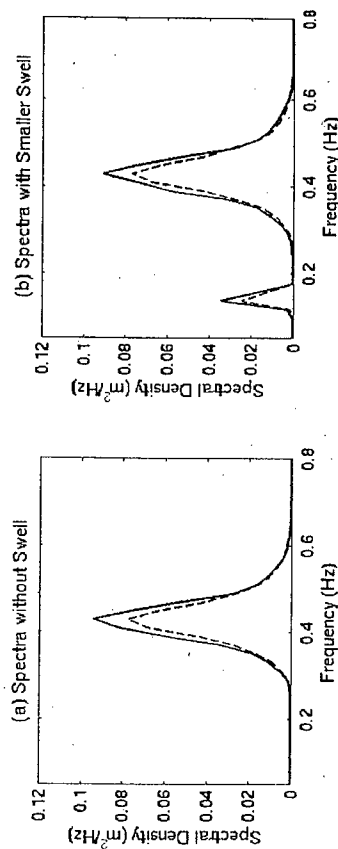
Figure 9. Suppression of wave growth by the swell (left) with a small amplitude. Dashed lines: up-wave boundary, solid lines: 4 km down-wave.

The numerical results suggest that on the swell crests, the larger surface roughness and the sheltering effect lead to a larger momentum transfer than that on the swell trough, but the momentum/energy flux averaged over the swell wavelength remains relatively unchanged. The majority of the short waves riding on the swell crest are subjected to the swell-induced form drag owing to the sheltering effect and a homogeneous wind stress over an entire short wavelength prevents the short wave from growing. Therefore, the swell takes advantage of the stronger momentum flux on its crest and harvests most of the energy transferred from the wind to the water. In layman's words, the finite amplitude swell serves as a "master" wave and the wind waves riding on the swell act as "slaves" for momentum transfer. Consequently, the swell amplitude increases while the wind sea barely grows.

5. Summary and Conclusions

A phase-resolving wind stress formula has been developed, analyzed and applied. The paper documents (1) the parameterization of the momentum flux transferred from the wind to surface gravity waves in a phase-resolving Boussinesq wave model, (2) the analysis of the effect of wave nonlinearity on the drag coefficient based on Stokes' second-order wave theory, (3) tests of the extended Boussinesq model with the wind forcing against wave measurements in a shallow lake, and (4) numerical experiments on the influence of swell on the growth rate of the wind waves. Fairly good agreement between the modeled wave heights and field data has been found. A new, simple mechanism has been suggested to explain the suppression of the wind wave growth rate in the presence of swell.

The methodology for the parameterization of the phase-resolving air-sea momentum flux as well as the extended Boussinesq wave model incorporating the wind effects appear to be a promising tool for the study of sea-swell-wind

GROWTH RESPONSE OF WAVES TO THE WIND STRESS

WILLIAM L. PEIRSON

Water Research Laboratory, School of Civil and Environmental Engineering, University of New South Wales, King St., Manly Vale NSW 2093, AUSTRALIA

STEPHEN E. BELCHER

Department of Meteorology, University of Reading, Earley Gate, P.O. Box 243 Reading RG6 6BB, UNITED KINGDOM

A re-analysis wave growth data available in the literature has been undertaken during this study. Data from the sources used by Plant (1982) have been assembled and supplemented by substantial data sets from six other sources. These data sets show growth rates compatible with Plant's curve only if Plant's uncertainty factor of 2 is retained. We have found systematic wave growth behaviour when wave growth is normalised by wave speed multiplied by total wind stress and then plotted as a function of the mean wave steepness. Wave energy input increases approximately quadratically with mean wave steepness to the point of initiation of both breaking and flow separation. Across the transition to breaking, there is no further increase in normalised wave energy input but for strong breaking, no other measurements are available at present. Net wave attenuation rates in the presence of an opposing wind are much greater than wave growth rates for comparable forcing once the mean steepness exceeds approximately 0.05.

1. Introduction

Determining the wave climate is fundamental to analysis and design in the coastal environment. Unfortunately, the wind conditions responsible for the most severe coastal wave climates can be rarely approximated by a delineated fetch exposed to a unidirectional wind field. Consequently, nomograms of peak spectral wave height and period of wave fields based on measurements (e.g. USACE, 1984; Donelan, 1990; Young, 1999) must be applied with caution and considerable uncertainty. The most severe wave states are usually associated with cyclonic storms that are characterised by a moving core and rapidly turning wind fields. The wave climate radiated by these systems is critically dependent on the region of most intense wave generation which is close to the centre of the storm.

Investigations over the last 50 years have shown that predicting the design wave conditions associated with storms requires analysis of spectral response for directional components over a selected spatial domain. Numerical models of sea state development for variable surface wind fields have developed in complexity and capability since the pioneering work of Pierson, Neumann and James, 1955. More recent assessments of operational wave model capability in

Geernaert, G. L. (1990). Bulk parameterizations for the wind stress and heat fluxes. *Surface Waves and Fluxes*, Edited by G. L. Geernaert and W. J. Plant. Kluwer Academic Publishers. Vol. 1, 91-172.

Hwang, P. A. (1999). Microstructure of ocean surface roughness: A study of spatial measurement and laboratory investigation of modulation analysis. *J. Phys. Oceanography*, 16, 1619-1629.

Hwang, P. A. (2002). Phase distribution of small-scale ocean surface roughness. *J. Phys. Oceanography*, 32, 2977-2987.

Jeffreys, H. (1925). On the formation of waves by wind. II. *Proc. Roy. Soc. A*, 110, 341-347.

Jiang, L., Lin, H., Schultz, W. W., and Perlin, M., (1999). Unsteady ripple generation on steep gravity-capillary waves. *J. Fluid Mech.*, 386, 281-304.

Kennedy, A. B., Kirby, J. T., and Gobbi, M. F. (2002). Simplified higher-order Boussinesq equations I. Linear simplifications. *Coastal Engineering*, 44, 205-229.

Longuet-Higgins, M. S. and Stewart, R. W. (1960). Changes in the form of short gravity waves on long waves and tidal currents. *J. Fluid Mech.*, 8, 565-585.

Longuet-Higgins, M. S. (1963). The generation of capillary waves by steep gravity waves. *J. Fluid Mech.*, 16, 138-159.

Madsen, P. A., and Schaffer, H. A. (1998). Higher order Boussinesq-type equations: Derivation and analysis. *Philosophical Trans. Royal Soc.*, 356, 3123-3184.

Madsen, P. A., Bingham, H. B., and Liu, H. (2002). A new Boussinesq model for fully nonlinear waves from shallow to deep water. *J. Fluid Mech.*, 462, 1-30.

Schwab, D. J., Bennett, J. R., Liu, P. C., and Donelan, M. A. (1984). Application of a simple numerical wave prediction model to Lake Erie. *Journal Geophysical Research.* 89 (C3), 3586-3592.

Shi, F., Kirby, J. T., Dalrymple, R. A., and Chen, Q. (2003). Wave simulations in Ponce de Leon inlet using a Boussinesq model. *Journal of Waterway, Port, Coastal and Ocean Engineering.* 129, 124-135.

Taylor, P. K. and Yelland, M. J. (2001) The dependence of sea surface roughness on the height and steepness of the waves. *J. Phys. Oceanogr.* 31, 572-590.

Young, I. R and Verhagen, L. A. (1996). The growth of fetch limited waves in water of finite depth. Part 1: Total energy and peak frequency. *Coastal Engineering.* 29, 47-78.